Journal of Power Sources 185 (2008) 734–739

Contents lists available at ScienceDirect

Journal of Power Sources

journal homepage: www.elsevier.com/locate/jpowsour

Non-destructive transmission electron microscopy study of catalyst degradation under electrochemical treatment

Karl J.J. Mayrhofer[a,*], Sean J. Ashton[a], Josef C. Meier[a], Gustav K.H. Wiberg[a], Marianne Hanzlik[b], Matthias Arenz[a,**]

[a] Institut für Physikalische Chemie, Technische Universität München, Garching, D-85748, Germany
[b] Zentrum für Elektronenmikroskopie, Technische Universität München, Garching, D-85748, Germany

ARTICLE INFO

Article history:
Received 13 June 2008
Received in revised form 13 July 2008
Accepted 3 August 2008
Available online 13 August 2008

Keywords:
Fuel cell
Catalyst degradation
Transmission electron microscopy
Accelerated electrocatalyst testing

ABSTRACT

A novel, non-destructive transmission electron microscopy technique is introduced, which enables the observation of the identical locations of a catalyst before and after electrochemical treatment (IL-TEM). The significance of this method is exemplified by the analysis of a standard, commercially available carbon supported platinum catalyst. We demonstrate that the observed changes of the catalyst particles are a direct consequence of the applied electrochemical treatment; and that selected catalyst regions are representative for the catalyst as a whole. Different electrochemical treatments were applied in order to discuss the potential of the method for studying processes of catalyst degradation.

1. Introduction

Fundamental investigations of electrocatalysts are essential for the further development of practical applications such as fuel cells or batteries [1]. Besides the activity and selectivity for certain electrochemical reactions, the long term stability of the catalyst is of major interest. Whereas plenty of advances in the performance of catalysts have been recently reported [2–6], improvements in the durability are scarce. This is partially due to the lack of investigative techniques that enable an effective analysis of degradation processes in electrolyte solutions. Commonly, the loss of active surface area is determined in-situ by electrochemical means [7,8]. Additionally, X-ray diffraction (XRD) and transmission electron microscopy (TEM) are applied to obtain the average crystallite size and complete size distributions, respectively. Latter techniques are, however, considered destructive for the study of electrocatalysts [9], since the catalyst has to be removed from the working electrode after the treatment in electrolyte. Consequently, only one single measurement can be conducted on a certain sample, in contrast to in-situ ultra-high vacuum TEM studies of catalysts [10,11].

The information on the surface area loss and/or particle growth is often not sufficient for a detailed description of occurrences on the catalyst particles in the nanometer scale. As a consequence, several theories are proposed in order to explain the loss in the active surface area of catalysts. The four primary mechanisms believed to be of relevance to low temperature fuel cell catalysts are [12–15]: (i) *Ostwald-ripening*, metal ions dissolve from smaller particles, diffuse, and re-deposit onto larger particles, resulting in reduced metal surface area via a minimization in surface energy; (ii) *reprecipitation*, Pt dissolves into the ionomer phase within the cathode and then precipitates again as newly formed Pt particles via the reduction of hydrogen; (iii) *particle coalescence*, Pt particles that are in close proximity sinter together to form larger particles; (iv) *corrosion of the carbon support* that anchors the Pt particles and provides electrical contact. These particle growth mechanisms and their rates may vary as a function of electrode potential, cell voltage cycling conditions, current density, particle size and shape, the hydration state of the membrane, and operating conditions.

In order to obtain an improved understanding of the degradation mechanism of fuel cell catalysts, we developed a novel, non-destructive method based on TEM, which enables the investigation of identical locations on a catalyst before and after electrochemical treatments (IL-TEM). The results from studies on a standard, commercially available Pt catalyst presented in this work should demonstrate the high potential of this method.

* Corresponding author. Tel.: +49 8928913294; fax: +49 8928913389.
** Corresponding author.
E-mail addresses: karl.mayrhofer@mytum.de (K.J.J. Mayrhofer), matthias.arenz@mytum.de (M. Arenz).

0378-7753/$ – see front matter © 2008 Elsevier B.V. All rights reserved.
doi:10.1016/j.jpowsour.2008.08.003

2. Experimental

2.1. Electrochemical measurements

The electrochemical measurements were conducted in an all-Teflon three-compartment electrochemical cell [16], using a rotating disc electrode (RDE) setup (Radiometer Analytical, France) and potentiostat (Bank, Germany). A saturated calomel electrode (SCE), separated by an electrolytic bridge from the main cell compartment was used in each experiment. However, all potentials were calculated with respect to the reversible hydrogen potential (RHE), which was measured for every experiment. A graphite rod was used as counter electrode. The electrolyte was prepared using Millipore Milli-Q® water (>18.3 MΩ cm^{-1}, TOC < 5 ppb) and concentrated $HClO_4$ (Normatom; VWR, Germany).

The carbon supported catalyst with a 50.6 wt.% Pt content (Tanaka Kikinzoku Kogyo K. K., Japan) was dispersed ultrasonically in ultrapure water to a concentration of 0.28 $mg_{Catalyst}$ mL^{-1} for at least 30 min. Before each measurement the catalyst suspension was placed into an ultrasonic bath for 5 min. During ultrasonic dispersion, a volume of 20 μL of the suspension was pipetted onto a polished glassy carbon substrate (5 mm diameter, 0.196 cm^2 geometrical surface area) leading to a Pt loading of 14 μg_{Pt} cm^{-2} for the catalyst. After the evaporation of the water in a nitrogen stream, the thus prepared electrode tip was inserted into the RDE, transferred to the electrochemical cell, and immersed under potential control at 0.05 V_{RHE} in argon-saturated 0.1 mol L^{-1} $HClO_4$ solution. The potential was then continuously cycled between 0.05 and 1.0 V_{RHE} until a stable cyclovoltammogram was recorded. The CO-stripping behaviour was studied in CO-free Ar-purged solution, after adsorbing CO at a potential of 0.05 V_{RHE}. The oxidation of CO_{ad} starts at a potential of approximately 0.7 V_{RHE} (Fig. 1a), reaching a maximum at around 0.88 V_{RHE} before declining back to the capacitive current at 1.0 V_{RHE} after all of the CO has been removed. The electrochemical measurements on the RDE were performed before and after each treatment procedure.

2.2. Transmission electron microscopy

For the TEM investigations the catalyst suspension was diluted by a factor of 1:10. A gold finder grid (400 mesh; Plano, Germany) was coated with a conducting film of carbon. The hydrophilicity of the carbon film (which is necessary for a uniform distribution of the catalyst particles) develops during a glow discharge exposure to an Ar-plasma. After this pre-treatment, 5 μL of catalyst suspension was pipetted onto the gold finder grid. In order to keep the catalyst loading as low as possible (to avoid overlapping catalyst particles), the drop was delicately absorbed off the grid after approximately 10 s, using a tissue. The grid was dried, and then investigated using a JEM 100CX microscope (JEOL, Japan) with an accelerating voltage of 100 kV.

For evaluating the initial state of the catalyst, firstly certain locations of the as-prepared catalyst agglomerates were analysed on the gold finder grid. Then the grid was transferred to the electrochemical cell, contacted by a Pt wire, and immersed into the electrolyte as a working electrode. After the electrochemical treatment, the TEM grid was dried under a gentle argon stream and transferred back for the TEM analysis. By means of an alphabet index, the identical quadrants on the grid were retrieved in the microscope with a thousand fold magnification. Within these quadrants, the identical catalyst agglomerates observed before treatment were again investigated using a magnification of 100*k*.

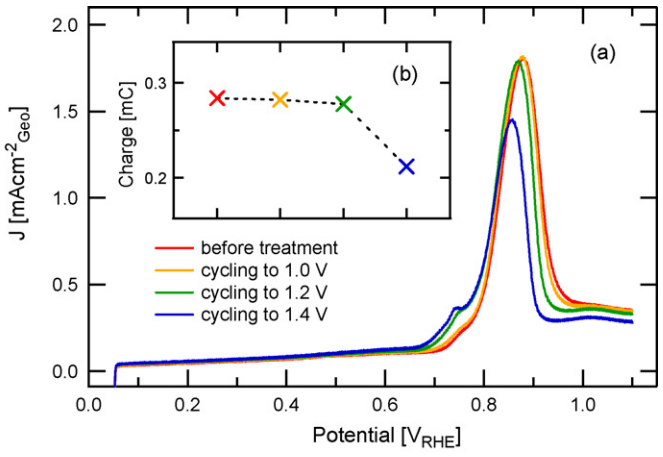

Fig. 1. CO-stripping curves recorded with 20 mV s^{-1} before and after several potential cycling treatments (a). The treatments were 3600 cycles with 1.0 V s^{-1} from a fixed, lower potential limit of 0.4 to 1.0 V_{RHE} (yellow), to 1.2 V_{RHE} (green) and to 1.4 V_{RHE} (blue). The integrated charges of the peaks are depicted in inset (b) (For interpretation of the references to colour in this figure legend, the reader is referred to the web version of the article).

2.3. Electrochemical treatment procedure

The electrochemical treatment procedure was performed in a separate three-compartment cell, using the same potentiostat and experimental setup as described for the RDE measurements. However, instead of using a single working electrode, two working electrodes were connected in parallel, namely the RDE and the TEM gold grid. Each were positioned in the electrochemical cell in such a way that the distance to the Luggin capillary, as well as to the counter electrode was equal in both cases. Both were connected over the same lead to the potentiostat, and were consequently subject to the same potential treatment. After the electrochemical treatment the RDE was transferred back into the measurement cell, whereas the TEM grid was subject to further TEM analysis.

3. Results

3.1. Proof of principle

A prerequisite for the new methodology is that the catalyst agglomerates on the TEM grid are not affected by the transfer procedure from the TEM microscope into the electrochemical cell and back. The observations should solely reflect the impact of the electrochemical treatment. Consequently, as a first step the influence of different electrochemical treatments on the catalyst was probed using the thin-film RDE method. In order to identify changes in the state of the catalyst, CO-stripping curves as well as cyclovoltammograms in argon-purged electrolyte were recorded before and after several different treatment procedures. The CO-stripping curves in Fig. 1 demonstrate the degradation of the active Pt surface area depending on the positive potential limit during cycling of the potential.

The red CO-stripping curve in Fig. 1 was recorded before the electrochemical treatment procedure. The orange, green and blue curves were received after cycling the potential 3600 times with 1.0 V s^{-1} between a lower potential limit of 0.4 V_{RHE} and an upper limit of 1.0, 1.2 and 1.4 V_{RHE}, respectively. These treatments ensured an alteration between a reduced surface state of Pt at 0.4 V_{RHE} and a state at which the Pt particles are oxidized to various degrees [17]. After scanning to 1.0 V_{RHE} the CO-stripping peak potential does not change, and the integrated charge under the peak decreases by less than 1% (Fig. 1b). If, however, the potential is cycled to 1.2 V_{RHE},

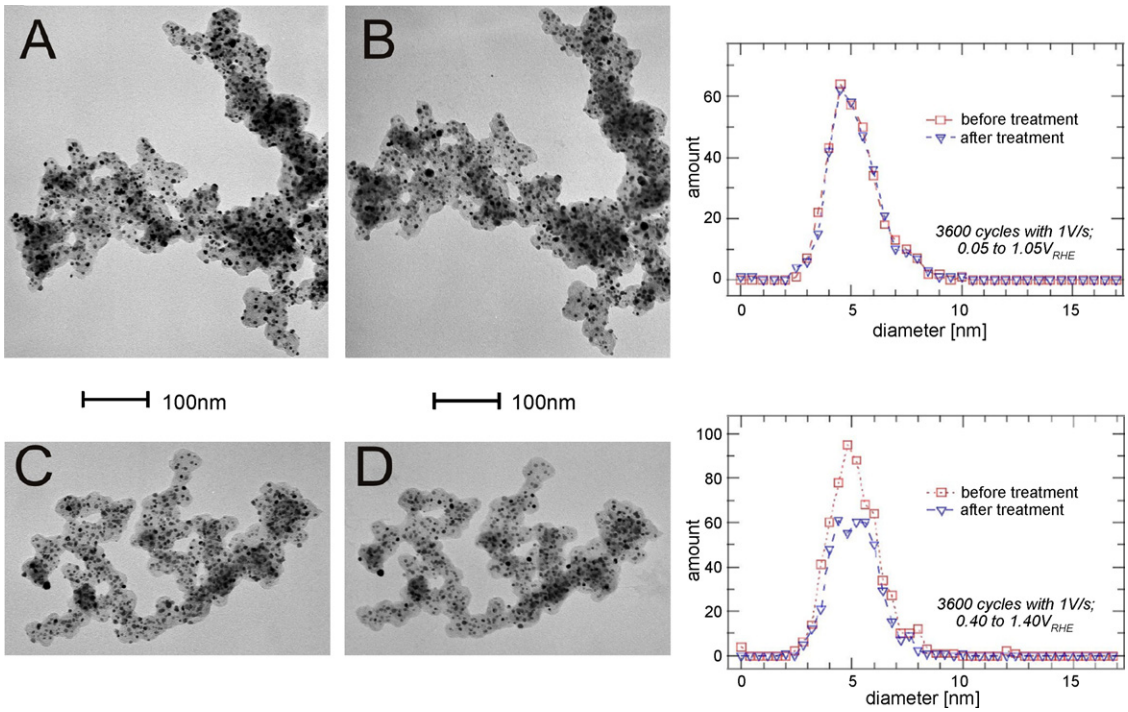

Fig. 2. IL-TEM micrographs recorded with a magnification of 100 k of the catalyst before (A + C) and after electrochemical treatment (B + D) in 0.1 mol L^{-1} $HClO_4$. The electrochemical treatment between A and B was 3600 cycles with 1.0 V s^{-1} in the potential region of 0.05 and 1.05 V_{RHE}, between C and D in the potential region of 0.40 and 1.4 V_{RHE}. The according Pt particle size distributions are depicted next to the corresponding images (including data from several other micrographs).

the CO-stripping peak shifts to negative potentials by 15 mV and a small pre-peak evolves. The latter observation is most likely due to the formation of defect sites on the Pt particles, which facilitate CO oxidation [18]. The peak shifts further negative by 10 mV after a potential cycling treatment up to 1.4 V_{RHE}. Moreover, the peak area dramatically declines, which also becomes visible in the inset (Fig. 1b). The decrease in the CO-stripping charge is a consequence of a diminished active surface area of Pt, a clear indication for the degradation of the catalyst.

Based on these results two different treatment conditions were chosen for the IL-TEM investigations; whereby one treatment causes no change of the catalyst, and another treatment in which a pronounced change is expected. As demonstrated in Fig. 2, in both experiments the identical catalyst agglomerates could be retrieved on the TEM grid.

The specific shape of the light grey carbon support in micrographs A and C before treatment can be relocated after electrochemical treatment, as evident in micrographs B and D,

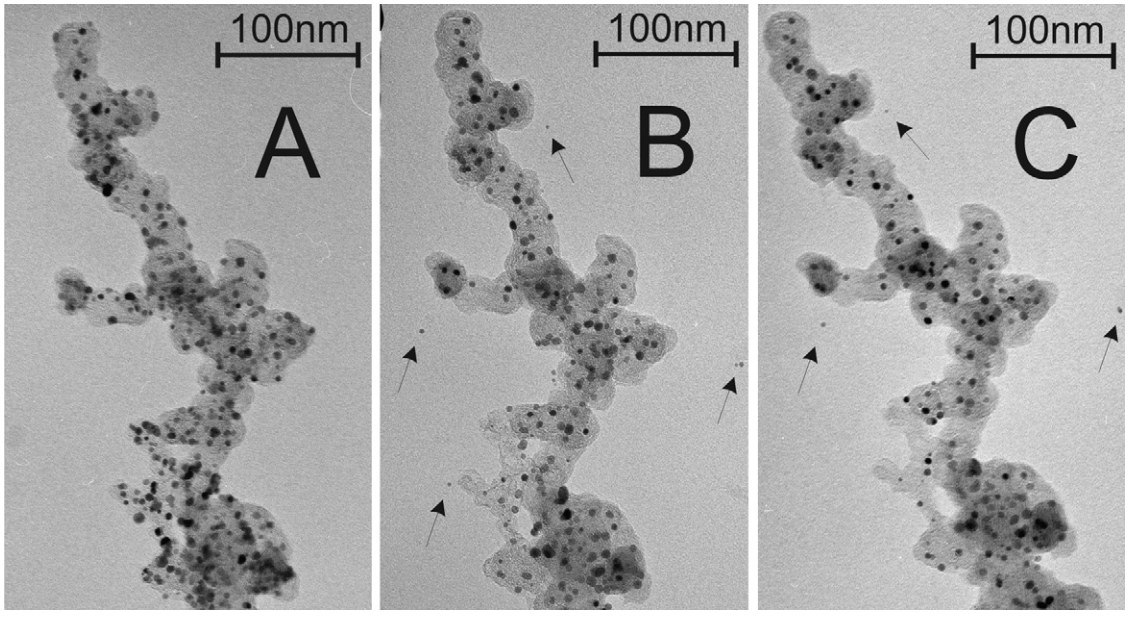

Fig. 3. IL-TEM micrographs (100 k) of a catalyst region before 3600 potential cycles between 0.4 and 1.4 V_{RHE} with 1 V s^{-1} (A), afterwards (B), and after another 3600 cycles (C) in 0.1 mol L^{-1} $HClO_4$; showcasing the detachment of Pt particles from the carbon support.

respectively. The Pt particles are visible as dark grey/black dots and posses a narrow size distribution ranging from 3 to 8 nm. They are distributed evenly on the support, a clear indication for the quality of the catalyst. Most importantly, in Fig. 2A and B it is evident that the electrochemical treatment as probed by the RDE (3600 cycles at 1.0 V s^{-1} in the region of 0.05 and 1.05 V_{RHE} at room temperature) appears to have little impact on the catalyst sample. When investigated in more detail, it becomes clear that the Pt particles stay at an identical location on the support. Additionally, their size does not vary, which is also displayed in the size distribution plot (Fig. 2). The numerical evaluation for this plot was performed on several identical, unambiguous and non-overlapping catalyst locations. In this context it should be emphasized that one of the major advantages IL-TEM offers compared to conventional TEM investigations of catalysts, is that both the size distributions and the absolute number of particles before and after treatment are directly comparable to each other.

A quite different picture develops for an electrochemical treatment in the potential range between 0.4 and 1.4 V_{RHE}, for which already significant changes were observed in the CO-stripping measurements. Although the carbon support retains its structure and shape, distinct variations occur for the Pt particles from micrograph C to D in Fig. 2. The most striking visible effect is the disappearance of whole particles from the support, which is also reflected in the size distribution plots for locations C and D. The amount of particles clearly diminishes for each particle size, however, the average particle size estimated from a Gaussian fit remains constant at 5.0 ± 0.1 nm.

In conclusion, the evaluation of micrograph A and B demonstrates that the transfer back and forth from IL-TEM analysis under vacuum conditions into an electrochemical cell can be accomplished without disturbing the catalyst's structure, which is a prerequisite for any further investigation. In addition, it was shown in micrographs C and D that IL-TEM is a powerful method for the visual study of the influence of (electro-) chemical treatment conditions on processes like catalyst degradation.

3.2. Particle detachment

In order to obtain accurate particle size distributions (as demonstrated in Fig. 2) and to draw conclusions on catalyst degradation mechanisms, individual Pt particles have to be observed in magnified IL-TEM micrographs. The enhancement of a particular catalyst location before (A), and after a first (B) and second (C) electrochemical treatment (potential cycling between 0.4 and 1.4 V_{RHE}) is presented in Fig. 3.

The disappearance of particles of various sizes from A to B to C can be visually observed, whereby the amount of particles decreases from 100% in A, to approximately 70% in B and 50% in C. Interestingly, the remaining particles remain unaltered in position and size, suggesting that particle agglomeration/movement plays a minor role under these specific treatment conditions. Furthermore, no preferential dissolution of small particles and growth of bigger particles appears to occur, as would be expected for an Ostwald-ripening type degradation. It seems particles simply detach as a whole from the support. A plausible explanation is that during

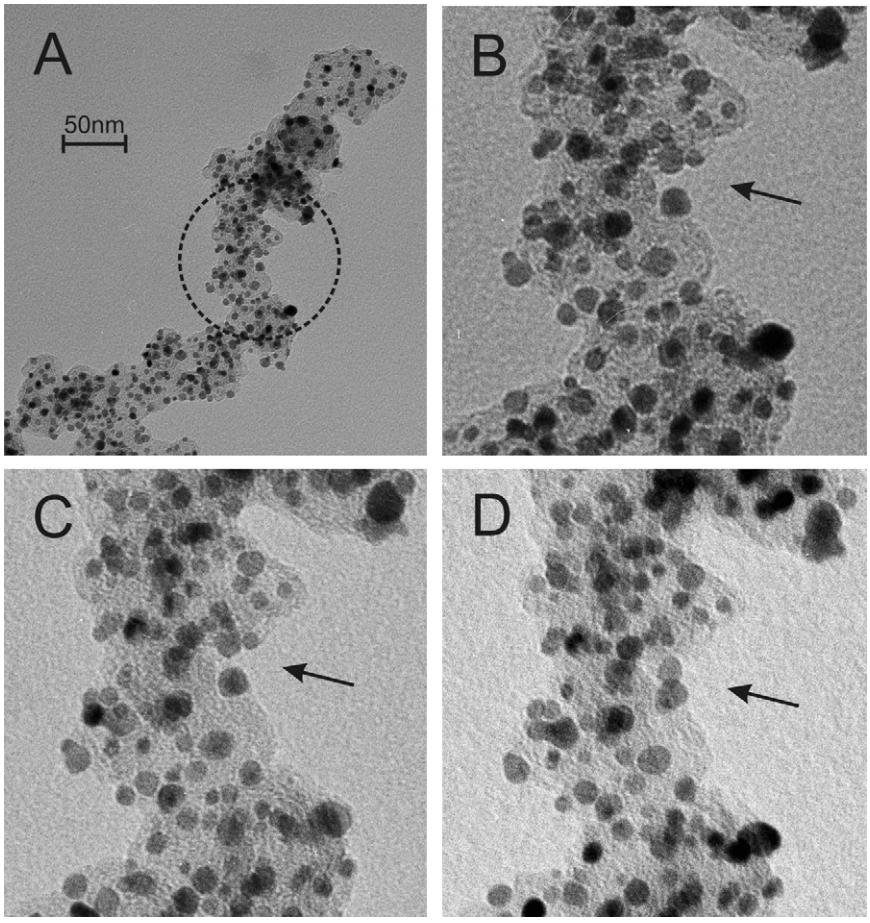

Fig. 4. IL-TEM micrographs with 100 k of a catalyst location before cycling (20 mV s^{-1}) between 0.05 and 0.65 V_{RHE} in CO-saturated 0.1 mol L^{-1} $HClO_4$ for 1 h (A + B), afterwards (C) and after another potential cycling treatment (20 mV s^{-1}) in Ar-purged 0.1 mol L^{-1} $HClO_4$ between 0.05 and 1.2 V_{RHE} for 1 h (D); the particle movement/agglomeration is indicated by the arrows.

potential cycling, a partial oxide layer forms between the Pt particles and the carbon support, leading to a gradual reduction in adhesion and finally to the complete detachment of particles [19]. The neutral Pt particles consequently disperse into the electrolyte, where they can be detected using ICP-OES. The Pt concentration in the electrolyte after the first treatment (21 ppb) and after the second treatment (22 ppb) is equivalent to approximately 20% particle loss, as expected from IL-TEM. In contrast, in the case of Ostwald-ripening Pt ions would re-deposit onto other Pt particles or the support below the standard reduction potential. This would lead to an increase in particle size or formation of new particles, which could not be observed.

It is important to note that the catalyst coverage on the TEM grid was below $\mu g\,cm^{-2}$ in order to be capable to unambiguously investigate individual particles. In actual applications with higher loadings it could be the case that detached particles do not dissolve into the electrolyte, but are instead physically trapped within the carbon support and can then re-deposit. An indication for this effect is given in Fig. 3B, in which four particles are clearly detached from the catalyst support, but have re-deposited on the carbon film of the TEM grid. Three of these Pt particles retain their position over the next electrochemical treatment and are also visible in image C. The exact extent of this effect is unclear, however, since no other cases of particle detachment and re-deposition other than in these particular micrographs were observed.

3.3. Particle movement and agglomeration

The detachment of whole particles was by far the governing process detected under harsh potential cycling conditions ($0.05–1.4\,V_{RHE}$). Under different treatment conditions, other effects can also be observed with IL-TEM. One specific case of particle movement and agglomeration is depicted in the micrographs in Fig. 4.

In this case, the catalyst on the TEM finder grid was subjected to a potential cycling treatment with $20\,mV\,s^{-1}$ in between 0.05 and $0.65\,V_{RHE}$ in CO-saturated $0.1\,mol\,L^{-1}$ $HClO_4$ solution for 1 h, a procedure that was applied in previous investigations [18]. After recording the intermediate TEM micrographs (image C), another treatment with $20\,mV\,s^{-1}$ in between 0.05 and $1.2\,V_{RHE}$ in Ar-purged electrolyte followed. A region of untreated catalyst encircled in image A is magnified in image B; image C and D represent the identical, magnified region after each electrochemical treatment, respectively. Again, no modification of the carbon support is observed. The Pt loading in this location is higher than in other locations, as can be anticipated from image A. Thus, plenty of particles are overlapping and an unambiguous analysis of the location for statistical purposes is not possible. In general, it seems that all particles remain unaltered throughout the treatments. An interesting phenomenon, however, can be seen upon close inspection of the three Pt particles on the edge of the support, indicated by the arrows in B, C and D. In image B and C all three are sufficiently separated to identify them as individual particles. Two are located above a small indent in the carbon support whilst the other is just below, with a gap of approximately 3 nm in between. In image D only one of the former particles is visible, indicating that either they have agglomerated, or the smaller particle has detached from the carbon support. It is clear, however, that the top particle moves away from its adjacent particles towards the bottom particle across the gap, to a point where they both overlap. At the same time, the remaining particles retain their position relative to each other, which is quite different to the displacement of the carbon support described in the upcoming section. Note that this effect only served to demonstrate the capabilities of IL-TEM, and might not be representative for the applied chemical treatment conditions.

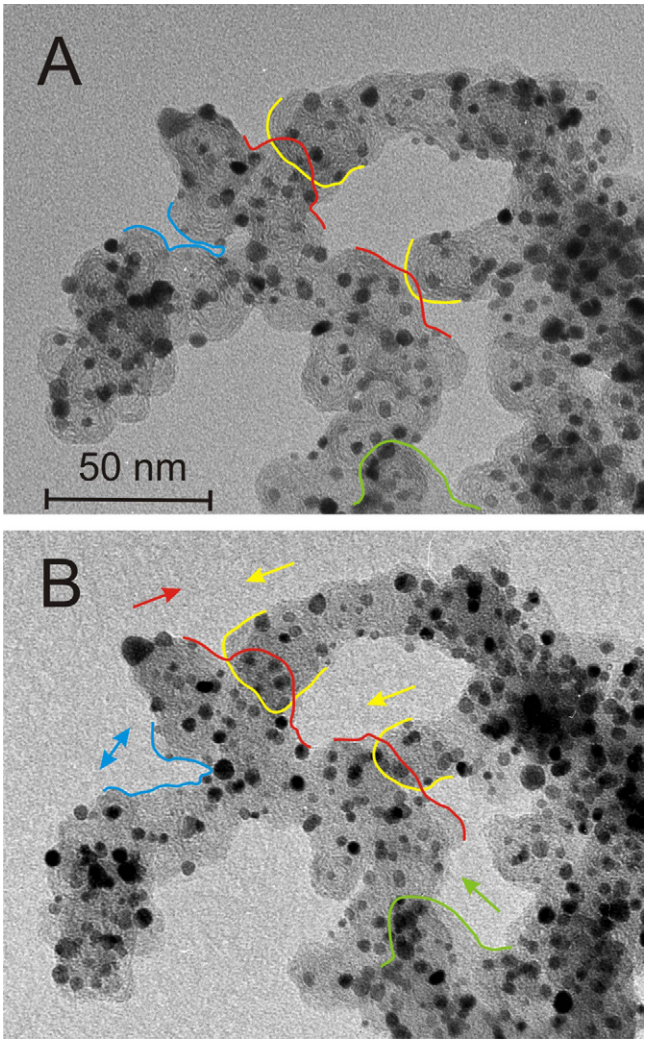

Fig. 5. IL-TEM image of a certain location on the catalyst before the electrochemical treatment described in Fig. 4(A) and afterwards (B). The coloured edges and arrows should aid to visualize the changes.

3.4. Displacement of the carbon support

The importance of a low loading for unambiguous, non-overlapping catalyst regions has already been mentioned in the context of the statistical analysis of particle features in Section 3.1. The reason why this is crucial for the proper interpretation of the IL-TEM micrographs is presented in Fig. 5.

Upon the electrochemical treatment described previously, the carbon catalyst support rearranged locally on the carbon film of the finder grid. This is indicated by the coloured edges in the images before (A) and afterwards (B). For clarity, the arrows indicate the direction of the displacement of the support. As a result, the yellow, red and green boundaries are more overlapping in image B, whereas the blue border becomes more separated. It appears that the catalyst is not sufficiently attached to the carbon film in order to stay exactly in place during the transfer from the TEM vacuum chamber to the acid solution and back. This becomes reasonable when we imagine the three-dimensional catalyst agglomerate structure that is depicted by the two-dimensional projection in the micrograph. Flakes of the catalyst support that are not in direct contact with

the carbon film could disengage while in solution; and dock back on again in a different configuration when gently dried afterwards. In this case, an unambiguous analysis of the overlapping regions would only be possible using 3D TEM [20,21]. Notice, however, that the displacement of the carbon support is an exceptional effect, like the particle movement/agglomeration in Section 3.3. In the majority of the micrographs the support is unmodified after the transfer, which enables the direct observation of corrosion processes of the nanoparticles on the support.

4. Summary and conclusion

We have demonstrated that IL-TEM is a powerful method enabling a direct, visual observation of the influence of electrochemical treatments on carbon supported high surface area catalyst. By utilizing a TEM gold finder grid as a support for a standard Pt fuel cell catalyst, identical locations of the catalyst are repeatedly retrieved, before and after different electrochemical treatments. Thus it was proved that the transfer itself from vacuum in the TEM to an electrolyte and back has no impact on the individual Pt particles. Only when the catalyst is subject to corrosive treatment, various changes such as particle detachment and particle movement/agglomeration can be observed. Special attention must be paid to the statistical analysis of the micrographs, since displacement of the carbon support in the course of the treatment can lead to overlapping catalyst regions that are not interpretable.

Acknowledgements

This work was supported by the DFG through the Emmy-Noether project ARE852/1-1. Karl J.J. Mayrhofer expresses his gratitude to the Austrian FWF, which supports him with an Erwin-Schrödinger Scholarship. We thank Dr. T. Tada of Tanaka Kikinzoku Kogyo K. K. for the supply of the catalysts.

References

[1] W. Vielstich, A. Lamm, H.A. Gasteiger, Handbook of Fuel Cells: Fundamentals, Technology, Applications, 3, Wiley, 2003.
[2] J. Zhang, M.B. Vukmirovic, Y. Xu, M. Mavrikakis, R.R. Adzic, Angew. Chem. Int. Ed. 44 (14) (2005) 2132–2135.
[3] S. Koh, J. Leisch, M.F. Toney, P. Strasser, J. Phys. Chem. C 111 (9) (2007) 3744–3752.
[4] H.A. Gasteiger, S.S. Kocha, B. Sompalli, F.T. Wagner, Appl. Catal. B: Environ. 56 (1–2) (2005) 9–35.
[5] V. Stamenkovic, B.S. Mun, K.J.J. Mayrhofer, P.N. Ross, N.M. Markovic, J. Rossmeisl, J. Greeley, J.K. Norskov, Angew. Chem. Int. Ed. 45 (18) (2006) 2897–2901.
[6] V.R. Stamenkovic, B. Fowler, B.S. Mun, G. Wang, P.N. Ross, C.A. Lucas, N.M. Markovic, Science 315 (5811) (2007) 493–497.
[7] T. Yoda, H. Uchida, M. Watanabe, Electrochim. Acta 52 (19) (2007) 5997–6005.
[8] K.J.J. Mayrhofer, D. Strmcnik, B.B. Blizanac, V. Stamenkovic, M. Arenz, N.M. Markovic, Electrochim. Acta 53 (7) (2008) 3181–3188.
[9] Z. Siroma, K. Ishii, K. Yasuda, M. Inaba, A. Tasaka, J. Power Sources 171 (2) (2007) 524–529.
[10] J.G. Lee, J. Lee, T. Tanaka, H. Mori, Phys. Rev. Lett. 96 (7) (2006) 075504.
[11] T. Akita, M. Okumura, K. Tanaka, M. Kohyama, M. Haruta, J. Mater. Sci. 40 (12) (2005) 3101–3106.
[12] R. Borup, J. Meyers, B. Pivovar, Y.S. Kim, R. Mukundan, N. Garland, D. Myers, M. Wilson, F. Garzon, D. Wood, P. Zelenay, K. More, K. Stroh, T. Zawodzinski, J. Boncella, J.E. McGrath, M. Inaba, K. Miyatake, M. Hori, K. Ota, Z. Ogumi, S. Miyata, A. Nishikata, Z. Siroma, Y. Uchimoto, K. Yasuda, K.I. Kimijima, N. Iwashita, Chem. Rev. 107 (10) (2007) 3904–3951.
[13] R.L. Borup, J.R. Davey, F.H. Garzon, D.L. Wood, M.A. Inbody, J. Power Sources 163 (1) (2006) 76–81.
[14] P.J. Ferreira, G.J. la O', Y. Shao-Horn, D. Morgan, R. Makharia, S. Kocha, H.A. Gasteiger, J. Electrochem. Soc. 152 (11) (2005) A2256–A2271.
[15] Y. Shao-Horn, W. Sheng, S. Chen, P. Ferreira, E. Holby, D. Morgan, Top. Catal. 46 (3) (2007) 285–305.
[16] K.J.J. Mayrhofer, G.K.H. Wiberg, M. Arenz, J. Electrochem. Soc. 155 (1) (2008) P1–P5.
[17] B.E. Conway, B. Barnett, H. Angerstein-Kozlowska, B.V. Tilak, J. Chem. Phys. 93 (11) (1990) 8361–8373.
[18] M. Arenz, K.J.J. Mayrhofer, V.R. Stamenkovic, B.B. Blizanac, T. Tada, N.M. Markovic, P.N. Ross, J. Am. Chem. Soc. 127 (18) (2005) 6819–6829.
[19] K.J.J. Mayrhofer, S.J. Ashton, G.K.H. Wiberg, F. Kraus, M. Hanzlik, M. Arenz, Electrochem. Commun. 10 (2008) 1144–1147.
[20] P.A. Midgley, M. Weyland, Ultramicroscopy 96 (3–4) (2003) 413–431.
[21] H. Jinnai, T. Ikehara, T. Nishi, Adv. Polym. Sci. 170 (2004) 115–167.